either an actual or implied endorsement of such products by the Department of Health and Human Services (DHHS). The following authors: M.E.T., G.H., T.N., E.R., D.C., and M.E. are employees of the U.S. Government and prepared this work as part of their official duties. Title 17, USC, § 105 provides that copyright protection under this title is not available for any work of the United States Government. Title 17, USC, § 101 defines a U.S. Government work as a work prepared by a military service member or employee of the U.S. Government as part of that person's official duties.
The American Academy of Ophthalmology Task Force for Developing Novel Endpoints for Premium Intraocular Lenses Members include Jack T. Holladay, MD, MSEE, Chair; Adrian Glasser, PhD, Scott MacRae, MD, Samuel Masket, MD, Walter Stark, MD, and the following Food and Drug Administration staff members: Malvina Eydelman, MD, Don Calogero, MS, Gene Hilmantel, OD, Eva Rorer, MD, Tieuvi Nguyen, PhD, and Michelle E. Tarver, MD, PhD.

Correspondence:
Flora Lum, MD, American Academy of Ophthalmology, Division of Quality and Data Science, 655 Beach Street, San Francisco, CA 94109-1336. E-mail: flum@aao.org.

Appendix 1. Oval Pupil Measurement Background and Standard Operating Procedure

Background

The only study of the oval pupil available was by Isotani et al[3] in 1995, who studied the ratio of the major to minor diameter in healthy subjects by using infrared photography. The subjects were dark adapted, so these are scotopic pupil measurements.

Standard Operating Procedure

If the clinician observes an oval or irregularly shaped pupil (dyscoria) at any visit after surgery, photographs should be taken at that visit and each subsequent visit to determine if the ovalization is progressive. The major and minor diameters of the pupil, which may not be orthogonal, are measured on the photograph, which must be taken in photopic conditions (>200 foot-candles or 2153 lux) so the pupil is maximally constricted. The pupil constriction provides the setting for pupil ovalization. For the measurement, the diameters must pass through the center of the least-squares, best-fit ellipse or centroid of the pupil perimeter. The ratio of the major to minor diameter is then calculated and reported. The photograph may be taken with any camera, including but not limited to slit-lamp cameras, topographers, and Scheimpflug devices, but the eye image must be captured under photopic conditions as specified.

References

1. Stark WJ, Worthen DM, Holladay JT, et al. The FDA report on intraocular lenses. *Ophthalmology*. 1983;90:311-317.
2. Lum F, Tarver ME, Kahook MY, et al. Special commentary: Food and Drug Administration and American Academy of Ophthalmology sponsored: developing novel endpoints for premium intraocular lenses workshop. *Ophthalmology*. 2015;122:1522-1531.
3. Isotani H, Fukumoto Y, Kitaoka H, et al. Oval pupil in patients with diabetes mellitus: examination by measurement of the dark-adapted pupillary area and pupillary light reflex. *Diabetes Res Clin Pract*. 1995;29:43-48.

Special Report: American Academy of Ophthalmology Task Force Summary Statement for Measurement of Tilt, Decentration, and Chord Length

Currently, the measurement of tilt and decentration is not commercially available in an instrument or method that has been validated clinically. In lieu of a validated, commercially available instrument or method, the current statuses of 3 different approaches that have been used to measure tilt and decentration are described to help provide the basis for the future development of an instrument or technique.

Definitions

- Decentration of an intraocular lens (IOL) is the lateral horizontal and vertical displacement of an IOL relative to the visual axis as seen by the clinician through the cornea (subject-fixated coaxially sighted corneal light reflex, as described by Chang and Waring[1]).
- Tilt of an IOL is the horizontal and vertical angle from perpendicular of an IOL relative to the visual axis (subject-fixated coaxially sighted corneal light reflex, as described by Chang and Waring[1]).
- Chord length μ is the displacement (distance) between the subject-fixated coaxially sighted corneal light reflex and pupil center.[1] For some diffractive IOLs, the midpoint between pupil center and visual axis may be optimal.

Tilt, Decentration, and Chord Length μ

The goal is to measure tilt, apparent decentration through the cornea, and chord length μ on all subjects with a premium IOL.

Table 1. Ratio of IOL Toricity to Corneal Astigmatism

	Effective Lens Position					
A-constant—>	116.346	117.203	118.059	118.916	119.773	120.630
Surgeon Factor—>	0.287	0.772	1.257	1.742	2.227	2.713
ELP—>	4.000	4.500	5.000	5.500	6.000	6.500
IOL Power	Resulting Ratio of IOL Toricity to 2 D of Corneal Astigmatism					
10	1.359	1.424	1.494	1.571	1.654	1.745
22	1.277	1.330	1.387	1.450	1.519	1.595
34	1.198	1.239	1.284	1.334	1.390	1.452
46	1.121	1.151	1.185	1.223	1.267	1.316

D = diopter; ELP = effective lens position; IOL = intraocular lens.

The 3 methods that have been used to measure 1 or more of these parameters are described next. In cases in which an investigator believes that the tilt has a clinically significant effect on a subject's vision, the induced astigmatism at the IOL plane should be calculated by taking into account the power of the implanted IOL and the tilt angle at the IOL plane (Appendix A, available at www.aaojournal.org). Apparent decentration >1.0 mm is equivalent to 1.7° of apparent tilt.[2]

Direct Measures of Tilt and Decentration

1. Using Purkinje images, effective lens position (ELP), and corneal curvature: The original description of measuring decentration and tilt using Purkinje images was by Phillips et al[3] in 1988. The patient fixates on a coaxial target with a telocentric camera. The image locations are used with the axial distances to the IOL surfaces and corneal curvature measurement to determine the tilt and decentration of the IOL. The Purkinje method has been substantiated many times over the past 20 years, the most recent of which was by Nishi et al[4] in 2010. Guyton et al[2] simplified the method using a penlight in 1990, but accuracy was sacrificed by having the clinician estimate the distance between images. Appendix B (available at www.aaojournal.org) describes a modification to enhance the precision of the method proposed by Guyton et al.[2]
2. Scheimpflug Imaging: In 2006, Rosales and Marcos[5] validated their Purkinje Imaging System, and in 2010, Rosales et al[6] compared Scheimpflug and Purkinje imaging. The Purkinje system images the reflections of an oblique collimated light source (in contrast to the coaxial light source described by Phillips et al[3]) on the anterior cornea and anterior and posterior IOL surfaces to determine the IOL tilt and decentration from the axial distance to the surfaces of the IOL and the corneal power. Scheimpflug imaging also requires geometric distortion correction and image processing techniques to retrieve the pupillary axis, IOL axis, and pupil center from the 3-dimensional anterior segment image of the eye.

Indirect Measure of Tilt at the Intraocular Lens Plane (May Be Used Only with Spherical Intraocular Lenses)

The vector difference between the net corneal astigmatism (front and back corneal surface) and the refractive astigmatism at the corneal plane is the lenticular (phakic or pseudophakic) astigmatism at the corneal plane, described in mathematical form as follows:

Net Corneal Astigmatism* + *Lenticular Astigmatism* = *Refractive Astigmatism

or

Lenticular Astigmatism* = *Refractive Astigmatism* − *Net Corneal Astigmatism

Because the ***Refractive Astigmatism*** of an eye has the opposite sign of the ***Refractive Error Astigmatism*** of the eye, the equation can be written:

Lenticular Astigmatism* = − *Refractive Error Astigmatism* − *Net Corneal Astigmatism

This equation describes the lenticular astigmatism at the corneal plane. If the vector differences are not oblique, the method for oblique cylinders between the keratometric and refractive error astigmatism is identical and completely described.[7]

If net corneal astigmatism or equivalent K-reading astigmatism[8] is not available, and only anterior surface K-readings are available, then the anterior surface K-reading may be modified to net corneal power by adding 0.22 diopters (D) at 180° (against-the-rule) vector to the anterior K-reading vector.[9,10] This would reduce with-the-rule by 0.22 D, increase against-the-rule by 0.22 D, and oblique astigmatism would be somewhere between, depending on the axis. According to the data in the 2 references, the resulting net corneal power will be within 0.25 D of the correct power 90% of the time.

The lenticular astigmatism needs to be converted from the corneal plane to the IOL plane. The conversion depends on the ELP and the power of the IOL. The exact conversion ratio can be determined postoperatively by using the spheroequivalent refraction, K-reading, axial length, and IOL power to calculate the actual ELP for a specific patient using Equations 13a−f on page 1367 in the article by Holladay.[11] By using the actual ELP and the actual IOL power, the exact ratio may be interpolated from Table 1 in the current article or calculated using the vergence formula by Holladay (Equation 2, page 1359).[11] Finally, the lenticular astigmatism at the IOL plane is used in Appendix A (available at www.aaojournal.org) along with the IOL power to estimate the tilt angle of the IOL.

Jack T. Holladay, MD, MSEE[1]
Don Calogero, MS[2]
Gene Hilmantel, OD[2]
Adrian Glasser, PhD[3]
Scott MacRae, MD[4]
Samuel Masket, MD[5]
Walter Stark, MD[6]
Michelle E. Tarver, MD, PhD[2]
Tieuvi Nguyen, PhD[2]
Malvina Eydelman, MD[2]

[1]*Department of Ophthalmology, Baylor College of Medicine, Houston, Texas;* [2]*Food and Drug Administration, Center for Devices and Radiological Health, Silver Spring, Maryland;* [3]*Independent Consultant, Tampa, Florida;* [4]*Flaum Eye Institute, University of Rochester, Rochester, New York;* [5]*Advanced Vision Care, Clinical Professor, David Geffen School of Medicine, Jules Stein Eye Institute, UCLA, Los Angeles, California;* [6]*Retired Distinguished Professor of Ophthalmology, Wilmer Eye Institute, Johns Hopkins University, Baltimore, Maryland*

Financial Disclosure(s): The author(s) have made the following disclosure(s): J.T.H.: Consultant − Abbott Medical Optics (Milpitas, CA); Alcon Laboratories, Inc. (Fort Worth, TX); Carl Zeiss, Inc. (Oberkochen, Germany); Oculus, Inc. (Wetzlar, Germany); Consultant and Equity Owner − AcuFocus, Inc. (Irvine, CA); ArcScan (Morrison, CO); Elenza (Roanoke, VA); Visiometrics (Barcelona, Spain).
A.G.: Consultant − Abbott Medical Optics, LensAR (Orlando, FL); Medicem (Cheshire, UK); Refocus Group (Dallas, TX); Tracey Technologies (Houston, TX); Vista Ocular (North Canton, OH); Consultant

and Equity Owner – Encore Vision (Fort Worth, TX); LensGen (Irvine, CA); PowerVision (Belmont, CA).
The mention of commercial products, their sources, or their use in connection with material reported herein is not to be construed as either an actual or implied endorsement of such products by the Department of Health and Human Services (DHHS). The following authors: M.E.T., G.H., T.N., E.R., D.C., and M.E. are employees of the U.S. Government and prepared this work as part of their official duties. Title 17, USC, § 105 provides that copyright protection under this title is not available for any work of the United States Government. Title 17, USC, § 101 defines a U.S. Government work as a work prepared by a military service member or employee of the U.S. Government as part of that person's official duties.
The American Academy of Ophthalmology Task Force for Developing Novel Endpoints for Premium Intraocular Lenses Members include Jack T. Holladay, MD, MSEE, Chair, Adrian Glasser, PhD, Co Chair, Scott MacRae, MD, Co Chair, Samuel Masket, MD, Walter Stark, MD, and the following Food and Drug Administration staff members: Malvina Eydelman, MD, Don Calogero, MS, Gene Hilmantel, OD, Eva Rorer, MD, Tieuvi Nguyen, PhD, and Michelle E. Tarver, MD, PhD.

Correspondence:
Flora Lum, MD, American Academy of Ophthalmology, Division of Quality and Data Science, 655 Beach Street, San Francisco, CA 94109-1336. E-mail: flum@aao.org.

References

1. Chang DH, Waring GO 4th. The subject-fixated coaxially sighted corneal light reflex: a clinical marker for centration of refractive treatments and devices. *Am J Ophthalmol*. 2014;158:863-874.
2. Guyton DL, Uozato H, Wisnicki HJ. Rapid determination of intraocular lens tilt and decentration through the undilated pupil. *Ophthalmology*. 1990;97:1259-1264.
3. Phillips P, Pérez-Emmanuelli J, Rosskothen HD, Koester CJ. Measurement of intraocular lens decentration and tilt in vivo. *J Cataract Refract Surg*. 1988;14:129-135.
4. Nishi Y, Hirnschall N, Crnej A, et al. Reproducibility of intraocular lens decentration and tilt measurement using a clinical Purkinje meter. *J Cataract Refract Surg*. 2010;36:1529-1535.
5. Rosales P, Marcos S. Phakometry and lens tilt and decentration using a custom-developed Purkinje imaging apparatus: validation and measurements. *J Opt Soc Am A Opt Image Sci Vis*. 2006;23:509-520.
6. Rosales P, De Castro A, Jiménez-Alfaro I, Marcos S. Intraocular lens alignment from Purkinje and Scheimpflug imaging. *Clin Exp Optom*. 2010;93:400-408.
7. Holladay JT, Cravy TV, Koch DD. Calculating the surgically induced refractive change following ocular surgery. *J Cataract Refract Surg*. 1992;18:429-443.
8. Holladay JT, Hill WE, Steinmueller A. Corneal power measurements using Scheimpflug imaging in eyes with prior corneal refractive surgery. *J Refract Surg*. 2009;25:862-868.
9. Koch DD, Ali SF, Weikert MP, et al. Contribution of posterior corneal astigmatism to total corneal astigmatism. *J Cataract Refract Surg*. 2012;38:2080-2087.
10. Savini G, Versaci F, Vestri G, et al. Influence of posterior corneal astigmatism on total corneal astigmatism in eyes with moderate to high astigmatism. *J Cataract Refract Surg*. 2014;40:1645-1653.
11. Holladay JT. Standardizing constants for ultrasonic biometry, keratometry, and intraocular lens power calculations. *J Cataract Refract Surg*. 1997;23:1356-1370.

Appendix A

APPENDIX A - INDUCED ASTIGMATISM (D) for TILT ANGLE (Degrees) versus IOL POWER (D) • VALUES > 2.0 D shaded in RED • Shaded YELLOW VALUE is example in TEXT

TILT ANGLE α	IOL Power (D)																																							
(Degrees)	1	2	3	4	5	6	7	8	9	10	11	12	13	14	15	16	17	18	19	20	21	22	23	24	25	26	27	28	29	30	31	32	33	34	35	36	37	38	39	40
1	0.00	0.00	0.00	0.00	0.00	0.00	0.00	0.00	0.00	0.00	0.00	0.00	0.00	0.00	0.00	0.00	0.01	0.01	0.01	0.01	0.01	0.01	0.01	0.01	0.01	0.01	0.01	0.01	0.01	0.01	0.01	0.01	0.01	0.01	0.01	0.01	0.01	0.01	0.01	0.01
2	0.00	0.00	0.00	0.00	0.01	0.01	0.01	0.01	0.01	0.01	0.01	0.01	0.02	0.02	0.02	0.02	0.02	0.02	0.02	0.02	0.03	0.03	0.03	0.03	0.03	0.03	0.03	0.03	0.04	0.04	0.04	0.04	0.04	0.04	0.04	0.04	0.05	0.05	0.05	0.05
3	0.00	0.01	0.01	0.01	0.01	0.02	0.02	0.02	0.02	0.03	0.03	0.03	0.04	0.04	0.04	0.04	0.05	0.05	0.05	0.05	0.06	0.06	0.06	0.07	0.07	0.07	0.07	0.08	0.08	0.08	0.09	0.09	0.09	0.09	0.10	0.10	0.10	0.10	0.11	0.11
4	0.00	0.01	0.01	0.02	0.02	0.03	0.03	0.04	0.04	0.05	0.05	0.06	0.06	0.07	0.07	0.08	0.08	0.09	0.09	0.10	0.10	0.11	0.11	0.12	0.12	0.13	0.13	0.14	0.14	0.15	0.15	0.16	0.16	0.17	0.17	0.18	0.18	0.19	0.19	0.20
5	0.01	0.02	0.02	0.03	0.04	0.05	0.05	0.06	0.07	0.08	0.08	0.09	0.10	0.11	0.12	0.12	0.13	0.14	0.15	0.15	0.16	0.17	0.18	0.18	0.19	0.20	0.21	0.21	0.22	0.23	0.24	0.25	0.25	0.26	0.27	0.28	0.28	0.29	0.30	0.31
6	0.01	0.02	0.03	0.04	0.06	0.07	0.08	0.09	0.10	0.11	0.12	0.13	0.14	0.16	0.17	0.18	0.19	0.20	0.21	0.22	0.23	0.24	0.26	0.27	0.28	0.29	0.30	0.31	0.32	0.33	0.34	0.35	0.37	0.38	0.39	0.40	0.41	0.42	0.43	0.44
7	0.02	0.03	0.05	0.06	0.08	0.09	0.11	0.12	0.14	0.15	0.17	0.18	0.20	0.21	0.23	0.24	0.26	0.27	0.29	0.30	0.32	0.33	0.35	0.36	0.38	0.39	0.41	0.42	0.44	0.45	0.47	0.48	0.50	0.52	0.53	0.55	0.56	0.58	0.59	0.61
8	0.02	0.04	0.06	0.08	0.10	0.12	0.14	0.16	0.18	0.20	0.22	0.24	0.26	0.28	0.30	0.32	0.34	0.36	0.38	0.40	0.42	0.44	0.46	0.48	0.50	0.52	0.54	0.56	0.58	0.60	0.62	0.64	0.66	0.68	0.70	0.72	0.74	0.76	0.78	0.80
9	0.03	0.05	0.08	0.10	0.13	0.15	0.18	0.20	0.23	0.25	0.28	0.30	0.33	0.35	0.38	0.40	0.43	0.46	0.48	0.51	0.53	0.56	0.58	0.61	0.63	0.66	0.68	0.71	0.73	0.76	0.78	0.81	0.83	0.86	0.89	0.91	0.94	0.96	0.99	1.01
10	0.03	0.06	0.09	0.13	0.16	0.19	0.22	0.25	0.28	0.31	0.35	0.38	0.41	0.44	0.47	0.50	0.53	0.57	0.60	0.63	0.66	**0.69**	0.72	0.75	0.79	0.82	0.85	0.88	0.91	0.94	0.97	1.00	1.04	1.07	1.10	1.13	1.16	1.19	1.22	1.26
11	0.04	0.08	0.11	0.15	0.19	0.23	0.27	0.31	0.34	0.38	0.42	0.46	0.50	0.54	0.57	0.61	0.65	0.69	0.73	0.76	0.80	0.84	0.88	0.92	0.96	0.99	1.03	1.07	1.11	1.15	1.19	1.22	1.26	1.30	1.34	1.38	1.41	1.45	1.49	1.53
12	0.05	0.09	0.14	0.18	0.23	0.27	0.32	0.37	0.41	0.46	0.50	0.55	0.60	0.64	0.69	0.73	0.78	0.82	0.87	0.92	0.96	1.01	1.05	1.10	1.15	1.19	1.24	1.28	1.33	1.37	1.42	1.47	1.51	1.56	1.60	1.65	1.70	1.74	1.79	1.83
13	0.05	0.11	0.16	0.22	0.27	0.33	0.38	0.43	0.49	0.54	0.60	0.65	0.70	0.76	0.81	0.87	0.92	0.98	1.03	1.08	1.14	1.19	1.25	1.30	1.35	1.41	1.46	1.52	1.57	1.63	1.68	1.73	1.79	1.84	1.90	1.95	2.01	2.06	2.11	2.17
14	0.06	0.13	0.19	0.25	0.32	0.38	0.44	0.51	0.57	0.63	0.70	0.76	0.82	0.89	0.95	1.01	1.08	1.14	1.20	1.27	1.33	1.39	1.46	1.52	1.58	1.65	1.71	1.77	1.84	1.90	1.96	2.03	2.09	2.15	2.22	2.28	2.34	2.41	2.47	2.54
15	0.07	0.15	0.22	0.29	0.37	0.44	0.51	0.59	0.66	0.73	0.81	0.88	0.95	1.03	1.10	1.17	1.25	1.32	1.39	1.47	1.54	1.61	1.69	1.76	1.83	1.91	1.98	2.06	2.13	2.20	2.28	2.35	2.42	2.50	2.57	2.64	2.72	2.79	2.86	2.94
16	0.08	0.17	0.25	0.34	0.42	0.51	0.59	0.67	0.76	0.84	0.93	1.01	1.10	1.18	1.26	1.35	1.43	1.52	1.60	1.69	1.77	1.85	1.94	2.02	2.11	2.19	2.28	2.36	2.44	2.53	2.61	2.70	2.78	2.87	2.95	3.03	3.12	3.20	3.29	3.37
17	0.10	0.19	0.29	0.38	0.48	0.58	0.67	0.77	0.87	0.96	1.06	1.15	1.25	1.35	1.44	1.54	1.63	1.73	1.83	1.92	2.02	2.11	2.21	2.31	2.40	2.50	2.60	2.69	2.79	2.88	2.98	3.08	3.17	3.27	3.36	3.46	3.56	3.65	3.75	3.85
18	0.11	0.22	0.33	0.44	0.54	0.65	0.76	0.87	0.98	1.09	1.20	1.31	1.42	1.53	1.63	1.74	1.85	1.96	2.07	2.18	2.29	2.40	2.51	2.61	2.72	2.83	2.94	3.05	3.16	3.27	3.38	3.49	3.59	3.70	3.81	3.92	4.03	4.14	4.25	4.36
19	0.12	0.25	0.37	0.49	0.61	0.74	0.86	0.98	1.10	1.23	1.35	1.47	1.60	1.72	1.84	1.96	2.09	2.21	2.33	2.46	2.58	2.70	2.82	2.95	3.07	3.19	3.31	3.44	3.56	3.68	3.81	3.93	4.05	4.17	4.30	4.42	4.54	4.66	4.79	4.91
20	0.14	0.28	0.41	0.55	0.69	0.83	0.96	1.10	1.24	1.38	1.51	1.65	1.79	1.93	2.06	2.20	2.34	2.48	2.62	2.75	2.89	3.03	3.17	3.30	3.44	3.58	3.72	3.85	3.99	4.13	4.27	4.40	4.54	4.68	4.82	4.96	5.09	5.23	5.37	5.51
21	0.15	0.31	0.46	0.61	0.77	0.92	1.08	1.23	1.38	1.54	1.69	1.84	2.00	2.15	2.30	2.46	2.61	2.77	2.92	3.07	3.23	3.38	3.53	3.69	3.84	4.00	4.15	4.30	4.46	4.61	4.76	4.92	5.07	5.22	5.38	5.53	5.69	5.84	5.99	6.15
22	0.17	0.34	0.51	0.68	0.85	1.03	1.20	1.37	1.54	1.71	1.88	2.05	2.22	2.39	2.56	2.73	2.90	3.08	3.25	3.42	3.59	3.76	3.93	4.10	4.27	4.44	4.61	4.78	4.96	5.13	5.30	5.47	5.64	5.81	5.98	6.15	6.32	6.49	6.66	6.83
23	0.19	0.38	0.57	0.76	0.95	1.14	1.33	1.51	1.70	1.89	2.08	2.27	2.46	2.65	2.84	3.03	3.22	3.41	3.60	3.79	3.98	4.17	4.36	4.54	4.73	4.92	5.11	5.30	5.49	5.68	5.87	6.06	6.25	6.44	6.63	6.82	7.01	7.20	7.38	7.57
24	0.21	0.42	0.63	0.84	1.05	1.25	1.46	1.67	1.88	2.09	2.30	2.51	2.72	2.93	3.14	3.35	3.56	3.76	3.97	4.18	4.39	4.60	4.81	5.02	5.23	5.44	5.65	5.86	6.07	6.27	6.48	6.69	6.90	7.11	7.32	7.53	7.74	7.95	8.16	8.37
25	0.23	0.46	0.69	0.92	1.15	1.38	1.61	1.84	2.07	2.30	2.53	2.76	3.00	3.23	3.46	3.69	3.92	4.15	4.38	4.61	4.84	5.07	5.30	5.53	5.76	5.99	6.22	6.45	6.68	6.91	7.14	7.37	7.60	7.83	8.06	8.29	8.52	8.75	8.99	9.22
26	0.25	0.51	0.76	1.01	1.27	1.52	1.77	2.02	2.28	2.53	2.78	3.04	3.29	3.54	3.80	4.05	4.30	4.56	4.81	5.06	5.32	5.57	5.82	6.07	6.33	6.58	6.83	7.09	7.34	7.59	7.85	8.10	8.35	8.61	8.86	9.11	9.37	9.62	9.87	10.12
27	0.28	0.55	0.83	1.11	1.39	1.66	1.94	2.22	2.50	2.77	3.05	3.33	3.61	3.88	4.16	4.44	4.72	4.99	5.27	5.55	5.83	6.10	6.38	6.66	6.94	7.21	7.49	7.77	8.05	8.32	8.60	8.88	9.16	9.43	9.71	9.99	10.27	10.54	10.82	11.10
28	0.30	0.61	0.91	1.21	1.52	1.82	2.12	2.43	2.73	3.03	3.34	3.64	3.95	4.25	4.55	4.86	5.16	5.46	5.77	6.07	6.37	6.68	6.98	7.28	7.59	7.89	8.19	8.50	8.80	9.10	9.41	9.71	10.02	10.32	10.62	10.93	11.23	11.53	11.84	12.14
29	0.33	0.66	0.99	1.33	1.66	1.99	2.32	2.65	2.98	3.31	3.64	3.98	4.31	4.64	4.97	5.30	5.63	5.96	6.30	6.63	6.96	7.29	7.62	7.95	8.28	8.61	8.95	9.28	9.61	9.94	10.27	10.60	10.93	11.27	11.60	11.93	12.26	12.59	12.92	13.25
30	0.36	0.72	1.08	1.44	1.81	2.17	2.53	2.89	3.25	3.61	3.97	4.33	4.69	5.06	5.42	5.78	6.14	6.50	6.86	7.22	7.58	7.94	8.31	8.67	9.03	9.39	9.75	10.11	10.47	10.83	11.19	11.56	11.92	12.28	12.64	13.00	13.36	13.72	14.08	14.44
31	0.39	0.79	1.18	1.57	1.96	2.36	2.75	3.14	3.54	3.93	4.32	4.72	5.11	5.50	5.89	6.29	6.68	7.07	7.47	7.86	8.25	8.65	9.04	9.43	9.82	10.22	10.61	11.00	11.40	11.79	12.18	12.57	12.97	13.36	13.75	14.15	14.54	14.93	15.33	15.72
32	0.43	0.85	1.28	1.71	2.14	2.56	2.99	3.42	3.84	4.27	4.70	5.12	5.55	5.98	6.41	6.83	7.26	7.69	8.11	8.54	8.97	9.39	9.82	10.25	10.68	11.10	11.53	11.96	12.38	12.81	13.24	13.66	14.09	14.52	14.95	15.37	15.80	16.23	16.65	17.08
33	0.46	0.93	1.39	1.85	2.32	2.78	3.24	3.71	4.17	4.63	5.10	5.56	6.02	6.49	6.95	7.41	7.88	8.34	8.81	9.27	9.73	10.20	10.66	11.12	11.59	12.05	12.51	12.98	13.44	13.90	14.37	14.83	15.29	15.76	16.22	16.68	17.15	17.61	18.07	18.54
34	0.50	1.00	1.51	2.01	2.51	3.01	3.52	4.02	4.52	5.02	5.53	6.03	6.53	7.03	7.54	8.04	8.54	9.04	9.55	10.05	10.55	11.05	11.55	12.06	12.56	13.06	13.56	14.07	14.57	15.07	15.57	16.08	16.58	17.08	17.58	18.09	18.59	19.09	19.59	20.10
35	0.54	1.09	1.63	2.18	2.72	3.26	3.81	4.35	4.90	5.44	5.98	6.53	7.07	7.62	8.16	8.70	9.25	9.79	10.34	10.88	11.43	11.97	12.51	13.06	13.60	14.15	14.69	15.23	15.78	16.32	16.87	17.41	17.95	18.50	19.04	19.59	20.13	20.67	21.22	21.76
36	0.59	1.18	1.77	2.35	2.94	3.53	4.12	4.71	5.30	5.89	6.48	7.06	7.65	8.24	8.83	9.42	10.01	10.60	11.18	11.77	12.36	12.95	13.54	14.13	14.72	15.31	15.89	16.48	17.07	17.66	18.25	18.84	19.43	20.01	20.60	21.19	21.78	22.37	22.96	23.55
37	0.64	1.27	1.91	2.55	3.18	3.82	4.45	5.09	5.73	6.36	7.00	7.64	8.27	8.91	9.55	10.18	10.82	11.46	12.09	12.73	13.36	14.00	14.64	15.27	15.91	16.55	17.18	17.82	18.46	19.09	19.73	20.36	21.00	21.64	22.27	22.91	23.55	24.18	24.82	25.46
38	0.69	1.38	2.06	2.75	3.44	4.13	4.81	5.50	6.19	6.88	7.56	8.25	8.94	9.63	10.31	11.00	11.69	12.38	13.06	13.75	14.44	15.13	15.81	16.50	17.19	17.88	18.56	19.25	19.94	20.63	21.31	22.00	22.69	23.38	24.06	24.75	25.44	26.13	26.81	27.50
39	0.74	1.48	2.23	2.97	3.71	4.45	5.20	5.94	6.68	7.42	8.17	8.91	9.65	10.39	11.13	11.88	12.62	13.36	14.10	14.85	15.59	16.33	17.07	17.82	18.56	19.30	20.04	20.78	21.53	22.27	23.01	23.75	24.50	25.24	25.98	26.72	27.47	28.21	28.95	29.69
40	0.80	1.60	2.40	3.20	4.01	4.81	5.61	6.41	7.21	8.01	8.81	9.61	10.41	11.21	12.02	12.82	13.62	14.42	15.22	16.02	16.82	17.62	18.42	19.23	20.03	20.83	21.63	22.43	23.23	24.03	24.83	25.63	26.43	27.24	28.04	28.84	29.64	30.44	31.24	32.04
41	0.86	1.73	2.59	3.46	4.32	5.18	6.05	6.91	7.78	8.64	9.50	10.37	11.23	12.10	12.96	13.83	14.69	15.55	16.42	17.28	18.15	19.01	19.87	20.74	21.60	22.47	23.33	24.19	25.06	25.92	26.79	27.65	28.51	29.38	30.24	31.11	31.97	32.83	33.70	34.56
42	0.93	1.86	2.80	3.73	4.66	5.59	6.52	7.45	8.39	9.32	10.25	11.18	12.11	13.04	13.98	14.91	15.84	16.77	17.70	18.63	19.57	20.50	21.43	22.36	23.29	24.22	25.16	26.09	27.02	27.95	28.88	29.82	30.75	31.68	32.61	33.54	34.47	35.41	36.34	37.27
43	1.00	2.01	3.01	4.02	5.02	6.03	7.03	8.04	9.04	10.04	11.05	12.05	13.06	14.06	15.07	16.07	17.07	18.08	19.08	20.09	21.09	22.10	23.10	24.11	25.11	26.11	27.12	28.12	29.13	30.13	31.14	32.14	33.15	34.15	35.15	36.16	37.16	38.17	39.17	40.18
44	1.08	2.17	3.25	4.33	5.41	6.50	7.58	8.66	9.74	10.83	11.91	12.99	14.07	15.16	16.24	17.32	18.40	19.49	20.57	21.65	22.73	23.82	24.90	25.98	27.06	28.15	29.23	30.31	31.39	32.48	33.56	34.64	35.72	36.81	37.89	38.97	40.05	41.14	42.22	43.30
45	1.17	2.33	3.50	4.67	5.83	7.00	8.17	9.33	10.50	11.67	12.83	14.00	15.17	16.33	17.50	18.67	19.83	21.00	22.17	23.33	24.50	25.67	26.83	28.00	29.17	30.33	31.50	32.67	33.83	35.00	36.17	37.33	38.50	39.67	40.83	42.00	43.17	44.33	45.50	46.67
46	1.26	2.51	3.77	5.03	6.29	7.54	8.80	10.06	11.32	12.57	13.83	15.09	16.34	17.60	18.86	20.12	21.37	22.63	23.89	25.15	26.40	27.66	28.92	30.17	31.43	32.69	33.95	35.20	36.46	37.72	38.98	40.23	41.49	42.75	44.00	45.26	46.52	47.78	49.03	50.29
47	1.36	2.71	4.07	5.42	6.78	8.13	9.49	10.84	12.20	13.55	14.91	16.26	17.62	18.97	20.33	21.68	23.04	24.39	25.75	27.10	28.46	29.81	31.17	32.52	33.88	35.23	36.59	37.94	39.30	40.65	42.01	43.36	44.72	46.07	47.43	48.78	50.14	51.49	52.85	54.20
48	1.46	2.92	4.38	5.84	7.30	8.76	10.22	11.68	13.14	14.61	16.07	17.53	18.99	20.45	21.91	23.37	24.83	26.29	27.75	29.21	30.67	32.13	33.59	35.05	36.51	37.97	39.43	40.89	42.36	43.82	45.28	46.74	48.20	49.66	51.12	52.58	54.04	55.50	56.96	58.42
49	1.57	3.15	4.72	6.30	7.87	9.45	11.02	12.60	14.17	15.75	17.32	18.90	20.47	22.04	23.62	25.19	26.77	28.34	29.92	31.49	33.07	34.64	36.22	37.79	39.37	40.94	42.51	44.09	45.66	47.24	48.81	50.39	51.96	53.54	55.11	56.69	58.26	59.83	61.41	62.98
50	1.70	3.40	5.09	6.79	8.49	10.19	11.89	13.58	15.28	16.98	18.68	20.38	22.08	23.77	25.47	27.17	28.87	30.57	32.26	33.96	35.66	37.36	39.06	40.75	42.45	44.15	45.85	47.55	49.24	50.94	52.64	54.34	56.04	57.74	59.43	61.13	62.83	64.53	66.23	67.92
51	1.83	3.66	5.50	7.33	9.16	10.99	12.82	14.66	16.49	18.32	20.15	21.98	23.82	25.65	27.48	29.31	31.14	32.98	34.81	36.64	38.47	40.30	42.14	43.97	45.80	47.63	49.46	51.30	53.13	54.96	56.79	58.62	60.46	62.29	64.12	65.95	67.78	69.62	71.45	73.28
52	1.98	3.95	5.93	7.91	9.89	11.86	13.84	15.82	17.80	19.77	21.75	23.73	25.71	27.68	29.66	31.64	33.61	35.59	37.57	39.55	41.52	43.50	45.48	47.46	49.43	51.41	53.39	55.37	57.34	59.32	61.30	63.28	65.25	67.23	69.21	71.18	73.16	75.14	77.12	79.09
53	2.14	4.27	6.41	8.54	10.68	12.81	14.95	17.08	19.22	21.35	23.49	25.63	27.76	29.90	32.03	34.17	36.30	38.44	40.57	42.71	44.84	46.98	49.12	51.25	53.39	55.52	57.66	59.79	61.93	64.06	66.20	68.33	70.47	72.61	74.74	76.88	79.01	81.15	83.28	85.42
54	2.31	4.62	6.92	9.23	11.54	13.85	16.15	18.46	20.77	23.08	25.39	27.69	30.00	32.31	34.62	36.92	39.23	41.54	43.85	46.15	48.46	50.77	53.08	55.39	57.69	60.00	62.31	64.62	66.92	69.23	71.54	73.85	76.16	78.46	80.77	83.08	85.39	87.69	90.00	92.31
55	2.50	4.99	7.49	9.98	12.48	14.97	17.47	19.97	22.46	24.96	27.45	29.95	32.45	34.94	37.44	39.93	42.43	44.92	47.42	49.92	52.41	54.91	57.40	59.90	62.40	64.89	67.39	69.88	72.38	74.87	77.37	79.87	82.36	84.86	87.35	89.85	92.34	94.84	97.34	99.83
56	2.70	5.40	8.10	10.81	13.51	16.21	18.91	21.61	24.31	27.02	29.72	32.42	35.12	37.82	40.52	43.22	45.93	48.63	51.33	54.03	56.73	59.43	62.14	64.84	67.54	70.24	72.94	75.64	78.34	81.05	83.75	86.45	89.15	91.85	94.55	97.26	99.96	102.66	105.36	108.06
57	2.93	5.85	8.78	11.71	14.64	17.56	20.49	23.42	26.34	29.27	32.20	35.13	38.05	40.98	43.91	46.83	49.76	52.69	55.62	58.54	61.47	64.40	67.32	70.25	73.18	76.11	79.03	81.96	84.89	87.81	90.74	93.67	96.60	99.52	102.45	105.38	108.30	111.23	114.16	117.08
58	3.18	6.35	9.53	12.70	15.88	19.05	22.23	25.40	28.58	31.75	34.93	38.10	41.28	44.45	47.63	50.80	53.98	57.15	60.33	63.50	66.68	69.85	73.03	76.20	79.38	82.55	85.73	88.90	92.08	95.25	98.43	101.60	104.78	107.95	111.13	114.30	117.48	120.65	123.83	127.00
59	3.45	6.90	10.34	13.79	17.24	20.69	24.14	27.59	31.03	34.48	37.93	41.38	44.83	48.27	51.72	55.17	58.62	62.07	65.52	68.96	72.41	75.86	79.31	82.76	86.20	89.65	93.10	96.55	100.00	103.45	106.89	110.34	113.79	117.24	120.69	124.13	127.58	131.03	134.48	137.93
60	3.75	7.50	11.25	15.00	18.75	22.50	26.25	30.00	33.75	37.50	41.25	45.00	48.75	52.50	56.25	60.00	63.75	67.50	71.25	75.00	78.75	82.50	86.25	90.00	93.75	97.50	101.25	105.00	108.75	112.50	116.25	120.00	123.75	127.50	131.25	135.00	138.75	142.50	146.25	150.00

Appendix B - Quantification of the Guyton Method

Background

The Guyton method[1] is a simple, rapid and accurate procedure for determining the tilt of an IOL **when the IOL is decentered less than 1 mm** (1mm produces 1.7° of apparent tilt and 2 mm 4.14° of apparent tilt). The procedure suggests the use of an arc scan perimeter which is unavailable to most practitioners at this time. The following procedure for taking measurements is recommended so that the angular tilt of an IOL in the absence of significant decentration may be determined.

Standard Operating Procedure

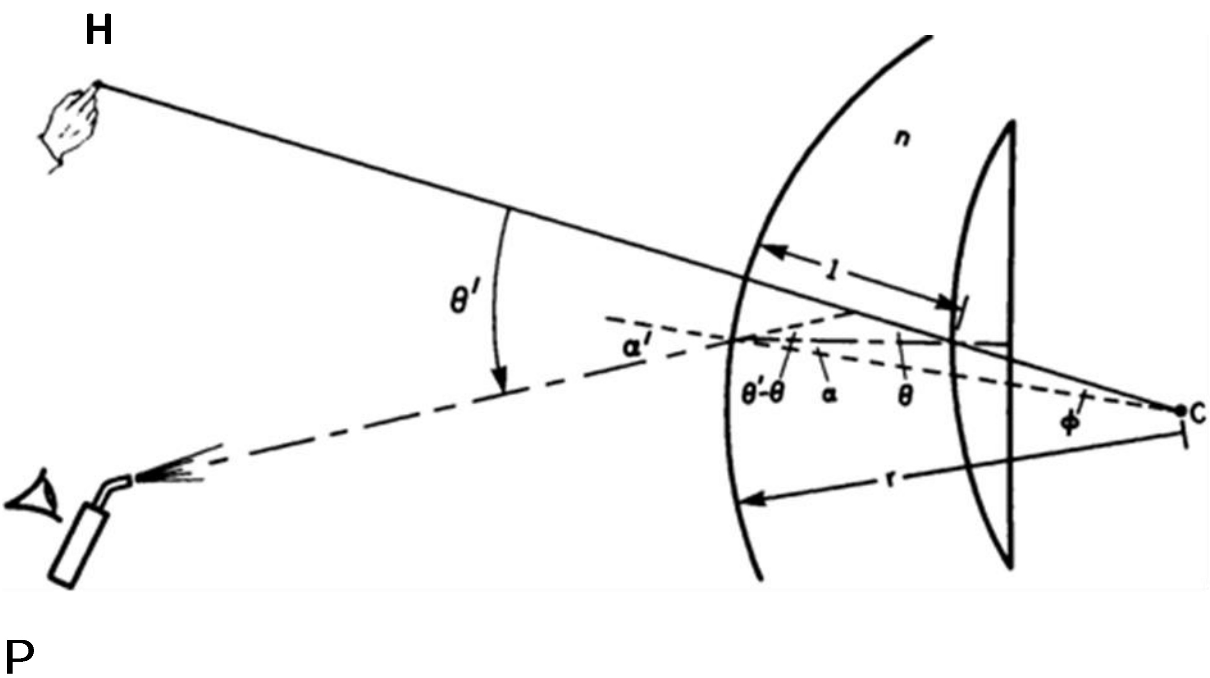

(Guyton Figure 8 modified). The IOL is tilted about its anterior vertex of the IOL and not decentered. The actual tilt (θ) can be shown in this case to be equal to approximately 0.85 times the apparent tilt (0.85 θ′). [For values from the Gullstrand schematic eye: n = 1.336, l = 3.6 mm, and r = 7.70 mm, θ = 0.85 θ′]

The triangle forming angle θ′ is formed by point V (vertex), point P (penlight) and point H (hand). Point V is about one-half of the depth of the anterior vertex of the IOL from the anterior vertex of the cornea and is ~ 4.5 mm for modern day posterior chamber IOLs in-the-bag, so would be ~ 2.2 mm. Since this distance is negligible relative to distances VP (nominally ~ 65 cm) and VH (nominally ~ 65 cm) it can be ignored. By measuring the distances VP, VH and PH angle θ may be determined.

From the Law of Cosines (Modified from Guyton to give exact angle θ)

$$HP^2 = VP^2 + VH^2 - 2\,VP\,VH\,\cos\theta'$$
$$\theta' = \cos^{-1}\left[\frac{VP^2 + VH^2 - HP^2}{2\,VP\;VH}\right]$$
$$\theta \cong 0.85\,\theta'$$

Example:

For VP = 65 cm, VH = 65 cm and HP = 10 cm

$$\theta' = \cos^{-1}\left[\frac{65^2 + 65^2 - 10^2}{2 \cdot 65 \cdot 65}\right]$$
$$\theta' = \cos^{-1}\left[\frac{8350}{8450}\right]$$
$$\theta' = 8.8235°$$
$$\theta \cong 7.4999°$$

The **direction of tilt** as mentioned by Davis, is the angle of the plane through the visual axis (PV in Figure 8 above) and is the same as the semi-meridians of the cornea (0° is left ear, 90° is superior, 180° is right ear and 270° is inferior).

DECENTRATION MEASUREMENT:

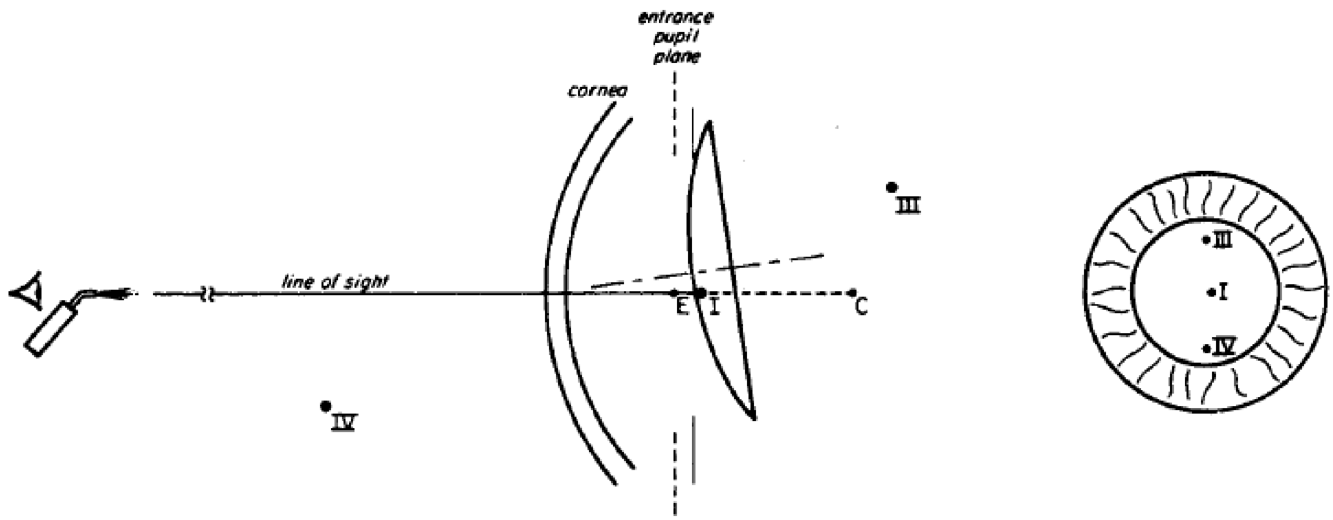

Figure 5 (From Guyton). Forward tilt and upward decentration of a forward-optic IOL (in this case convex-plano, but also is the same for a biconvex). The patient's line of sight passes from the center of the entrance pupil (E) to the fixation object (the hand light in this illustration). Purkinje images III and IV are displaced in opposite directions from the line of sight. Notice that the line connecting images III and IV is tilted approximately twice as much as the optical axis of the IOL, thus magnifying the apparent tilt of the IOL.

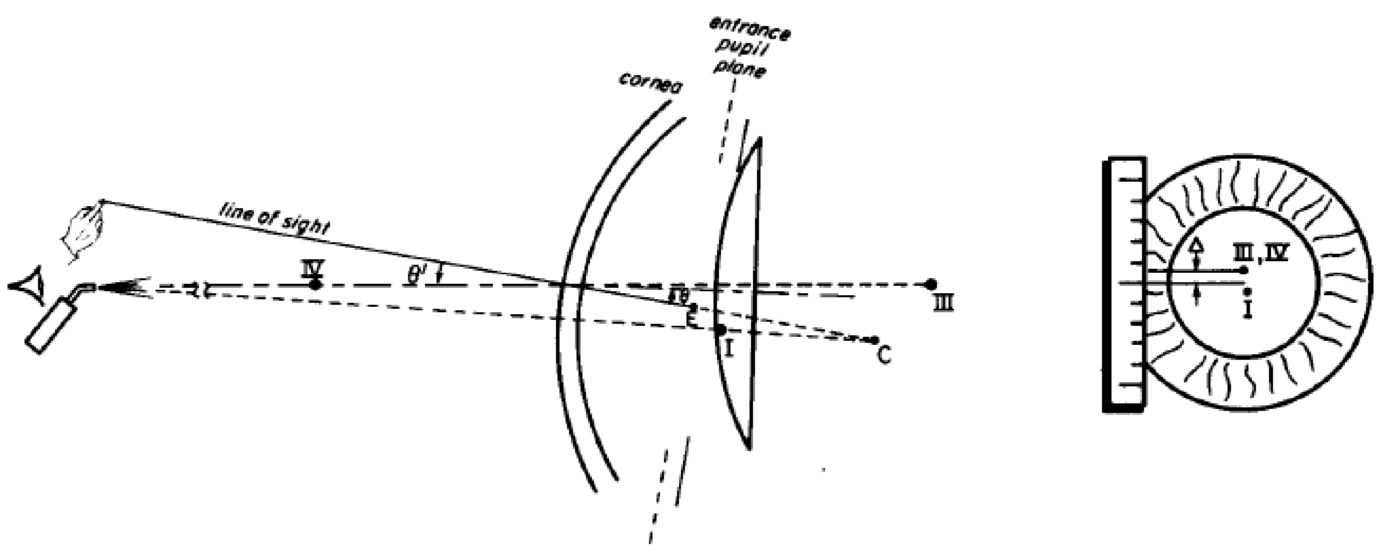

Figure 6 (From Guyton). With the patient looking at the examiner's finger, the examiner moves his finger in the frontal plane until Purkinje images III and IV, as sighted by the examiner's eye, become aligned with one another. The apparent IOL tilt (θ′) and decentration (Δ) are directly determined from this viewing situation.

In this example, the Purkinje images III and IV when superimposed are superior (90°) to Purkinje I and represent upward decentration. **The decentration may have a vertical and horizontal component such that the total decentration is the square root of the sum of the squares of the two components.**

Note: The Direction of Tilt may be from 0° to 359° for measuring θ'. The meridian about which the IOL is tilted is 90° from the Direction of Tilt and in the example above (Figure 6) is the 0° or 180° meridian or the horizontal. Also, the decentration is measured relative to Purkinje 1 (vertex normal and near visual axis), **not the center of the pupil**. An IOL will be considered perfectly centered when Purkinje I, III and IV are superimposable. This IOL will appear nasal (0.33 mm and slightly inferior) relative to the pupil center (angle Kappa or Lambda) or Chord Length Distance (µ) as defined by Chang and Waring.[11]

<u>A Simple Device for Quantitative Phaco-angulometry</u>

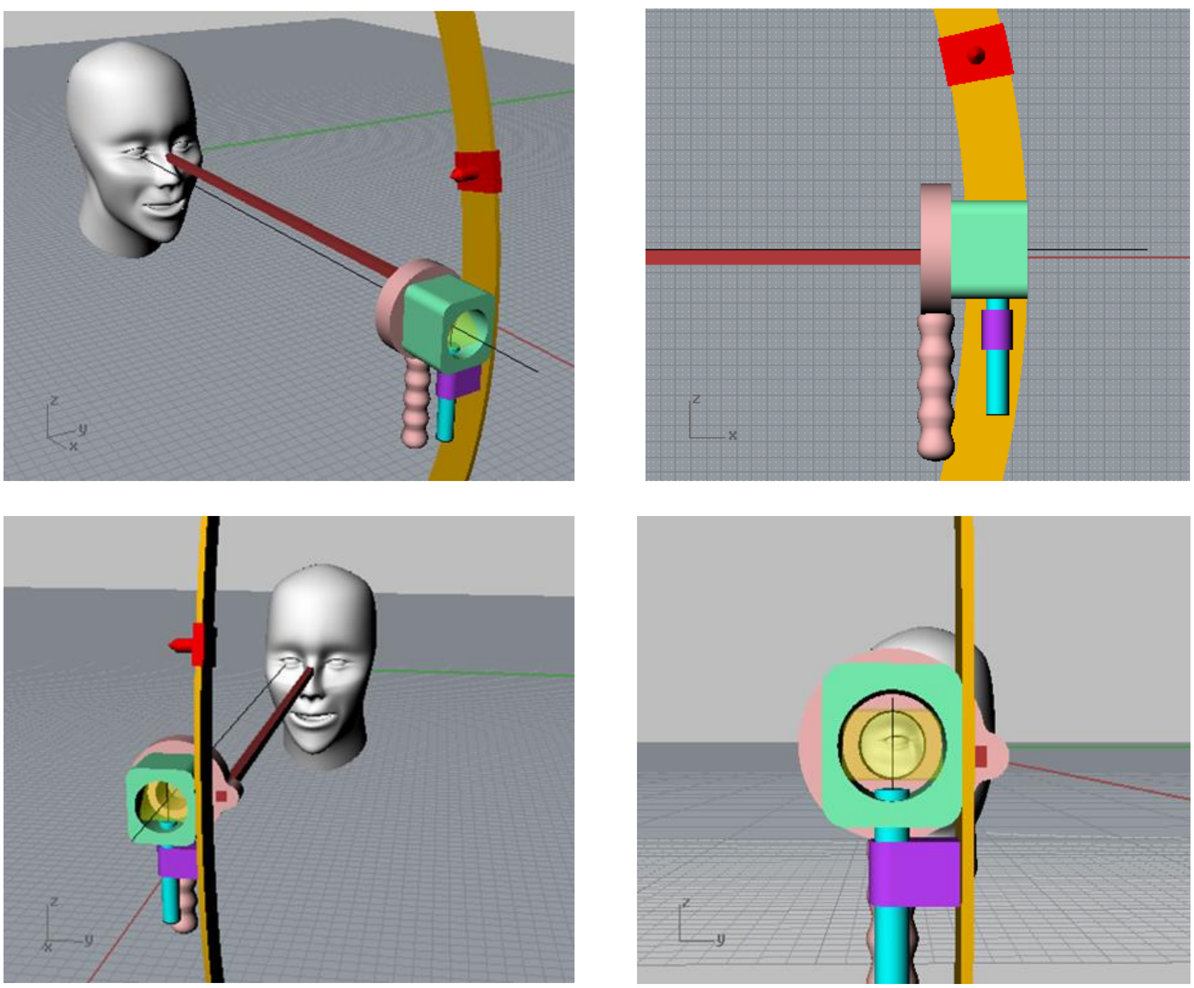

The images show the design of a simple, low cost device that could be used for phaco-angulometry. It consists of a handle (pink) with a hole through which the patient’s eye can be viewed by the examiner. To the handle is mounted a rotating cube (green) with a hole that houses a 45-degree angled beam splitter within, a pen-light below (blue) and an arc (gold) to the side. Light from the pen-light shines up and is reflected from the beam-splitter into the patient's eye. A sliding fixation target (red) is affixed to the arc. The center of curvature of the arc is at the vertex of the cornea. The arc is etched with degree markings. To the side of the handle is attached a light balsawood square dowel rod that is touched to the bridge of the patient’s nose to fix the working distance. With the patient looking at the fixation target, the examiner moves the fixation target along the arc and rotates the cube and arc until Purkinje images III and IV, as sighted by the examiner's eye, are aligned.